
This is an electronic reprint of the original article.
This reprint may differ from the original in pagination and typographic detail.

Sang, Yushuai; Li, Gen; Li, Xiang; Gong, Hanzhang; Yang, Mingze; Savary, David; Fei, Zhaofu; Dyson, Paul J.; Chen, Hong; Li, Yongdan

A synergistic approach for lignin biofuel production : Integrating non-catalytic solvolysis with catalytic product upgrading

Published in:
Chemical Engineering Journal

DOI:
[10.1016/j.cej.2024.153624](https://doi.org/10.1016/j.cej.2024.153624)

Published: 01/09/2024

Document Version
Publisher's PDF, also known as Version of record

Published under the following license:
CC BY

Please cite the original version:
Sang, Y., Li, G., Li, X., Gong, H., Yang, M., Savary, D., Fei, Z., Dyson, P. J., Chen, H., & Li, Y. (2024). A synergistic approach for lignin biofuel production : Integrating non-catalytic solvolysis with catalytic product upgrading. *Chemical Engineering Journal*, 495, Article 153624. <https://doi.org/10.1016/j.cej.2024.153624>

This material is protected by copyright and other intellectual property rights, and duplication or sale of all or part of any of the repository collections is not permitted, except that material may be duplicated by you for your research use or educational purposes in electronic or print form. You must obtain permission for any other use. Electronic or print copies may not be offered, whether for sale or otherwise to anyone who is not an authorised user.



A synergistic approach for lignin biofuel production: Integrating non-catalytic solvolysis with catalytic product upgrading

Yushuai Sang^a, Gen Li^a, Xiang Li^a, Hanzhang Gong^a, Mingze Yang^a, David Savary^b, Zhaofu Fei^b, Paul J. Dyson^b, Hong Chen^{c,*}, Yongdan Li^{a,*}

^a Department of Chemical and Metallurgical Engineering, School of Chemical Engineering, Aalto University, Kemistintie 1, Espoo, P.O. Box 16100, FI-00076, Finland

^b Institute of Chemical Sciences and Engineering, Swiss Federal Institute of Technology Lausanne (EPFL), 1015 Lausanne, Switzerland

^c School of Environmental Science and Engineering, Tianjin University, Tianjin 300072, China

ARTICLE INFO

Keywords:

Biorefinery
Biofuel
Catalytic upgrading
Enzymatic hydrolysis lignin
Non-catalytic solvolysis

ABSTRACT

Enzymatic hydrolysis lignin (EHL) is a large-scale industrial waste generated from the bio-ethanol production process. Its complex and heterogeneous nature as well as its low solubility in common solvents, has posed a persistent barrier to its effective utilization. Here, EHL was converted into biofuel through a two-step process, involving non-catalytic solvolysis followed by catalytic product upgrading. The non-catalytic solvolysis step achieved complete EHL liquefaction in a mixture of isopropanol and H₂O without char formation. In this step, H₂O disrupts the hydrogen bonds in EHL and isopropanol break π - π stacking interactions between the aromatic rings in EHL. H₂O also enhances EHL depolymerization, while isopropanol, as a hydrogen donor solvent, provides hydrogen that stabilizes active intermediates. In the catalytic product upgrading step, the liquid product of the first step was transformed into biofuels rich in cycloalkanes, arenes and alkylphenols, with a total carbon yield of 45.6 %. Isopropanol-H₂O reforming reactions provided hydrogen for the upgrading process, avoiding the introduction of H₂. This work demonstrates an effective approach for converting EHL into biofuels.

1. Introduction

Lignocellulose, comprising cellulose, hemicellulose, and lignin, is a sustainable feedstock with the potential to become the predominant renewable resource for producing commodity chemicals and fuels to achieve carbon-neutrality [1,2]. Nowadays, second-generation (2G) biorefineries using agricultural and forestry residues have been successfully built to convert cellulose and hemicellulose into bio-ethanol as a gasoline blend, but leaving lignin as a solid residue, named enzymatic hydrolysis lignin (EHL) [3]. For every litre of 2G bioethanol, 0.5–1.5 kg of EHL is produced depending on the lignin content in the original biomass used [3]. As a large scale industrial waste, EHL holds significant promise as a feedstock for producing biofuels to improve the sustainability and profitability of 2G biorefineries [3–5].

EHL solvolysis stands out as a promising method for depolymerizing EHL into high-value phenolics as biofuel precursors [6–10]. In our previous work, we depolymerized EHL in ethanol or methanol with different catalysts, including MoS₂ [11,12], unsupported Ni [13], NiMo/Al₂O₃ [14] and WO₃/Al₂O₃ [15], and achieved complete EHL

liquefaction and high yields of alkylphenols (20–30 wt%) at around 300 °C. In these reactions, catalysts play a crucial role in EHL liquefaction and phenolic monomer production [1,2,16–18]. Nevertheless, the utilization of a catalyst increases overall expenditure and the separation of the catalyst before product upgrading also introduces additional complexity and cost to the process. Non-catalytic lignin solvolysis, as a more economical process, has attracted significant attention [19–27]. These works explore the depolymerization of lignin into a lignin oil containing monomers and oligomers with only a solvent in the temperature range of 200–400 °C. However, repolymerization reactions of active intermediates occurs simultaneously with lignin depolymerization reactions, leading to a high yield of char typically in the range of 10–40 wt% [19–27]. The char formation remains the major challenge for non-catalytic lignin solvolysis.

The products obtained from EHL solvolysis exhibit high oxygen content, necessitating additional upgrading, particularly hydrodeoxygenation (HDO), to eliminate oxygen-containing functional groups and improve the heating values [28–30]. The HDO of lignin derived phenolics has been extensively investigated over the past two

* Corresponding authors.

E-mail addresses: chenhong_0405@tju.edu.cn (H. Chen), yongdan.li@aalto.fi (Y. Li).

<https://doi.org/10.1016/j.cej.2024.153624>

Received 22 February 2024; Received in revised form 8 June 2024; Accepted 29 June 2024

Available online 30 June 2024

1385-8947/© 2024 The Author(s). Published by Elsevier B.V. This is an open access article under the CC BY license (<http://creativecommons.org/licenses/by/4.0/>).

decades, resulting in the development of various catalysts, such as Ni and noble metal catalysts, Ni and Co-based phosphides, and Mo and W-based sulfides, carbides and oxides [31–33]. However, the HDO of lignin oil derived from solvolysis is more challenging due to the presence of large lignin fragments, which strongly adsorb onto the catalyst and hinder the HDO reaction [34]. To enhance HDO reaction and suppress char formation, high pressure of H₂ is typically introduced into the reaction [35]. Nevertheless, the storage and operation of high-pressure H₂ pose safety concerns to the overall process.

Herein, we developed a two-step process for producing biofuel from EHL, involving non-catalytic solvolysis followed by catalytic product upgrading. The non-catalytic EHL solvolysis was examined in methanol, ethanol, isopropanol and their mixtures with H₂O. Notably, complete EHL liquefaction was achieved in an isopropanol-H₂O mixture. The interactions between EHL and the solvents and the specific roles of isopropanol and H₂O in EHL liquefaction were investigated using operando HSQC-NMR spectroscopy and molecular dynamics simulations. The liquid product obtained was efficiently upgraded into biofuels rich in cycloalkanes, arenes and alkylphenols with isopropanol reforming reactions providing hydrogen, avoiding the introduction of extra H₂ gas.

2. Materials and methods

2.1. Materials

EHL was provided by Shandong Long Live biological technology Co., Ltd, and has been characterized in our previous work [36]. This type of EHL contains 91.2 wt% lignin, 1.42 wt% ash, and 0.12 wt% residual carbohydrate, and the weight percentages of C, O, H, N and S are 61.29, 29.61, 6.69, 0.98 and 0.01 wt%, respectively. The solvents (AR), including, isopropanol, ethanol and methanol, were purchased from VWR Chemicals. Deuterated solvents, including DMSO-*d*₆ (99.5 atom% D), isopropanol-*d*₈ (99.5 atom% D), and D₂O (99.8 atom% D), were purchased from Sigma-Aldrich. Raney Ni was also purchased from Sigma-Aldrich (Product Number: 221678).

2.2. Methods

2.2.1. Reaction conditions

Typically, 1 g of EHL combined with 50 mL of solvent was added into a 100 mL batch reactor (Kemi Co. Ltd, Hastelloy). The reactor underwent six purging cycles with N₂ to ensure an inert atmosphere. Subsequently, the reactor was heated to 250 °C and held at this temperature for 3 h with continuous stirring at 600 rpm. Following reaction, solid and liquid products are separated by filtration. The solid product, without undergoing any washing steps, was directly dried at 60 °C in a vacuum drying oven for 24 h. Subsequently, the weight of the dried solid product was measured using a balance and utilized to calculate the EHL liquefaction degree. The liquefaction degree was calculated with Eq. (1):

$$\text{Liquefaction degree (wt\%)} = \left(1 - \frac{\text{The weight of the solid residue}}{\text{The weight of added EHL}}\right) \times 100 \quad (1)$$

The liquid product was directly upgraded with 0.5 g of Raney Ni catalyst without solvent separation. The reaction was carried out at 320 °C for 6 h under N₂ in the same reactor, using the same procedure as the EHL liquefaction step. After reaction, the catalyst and liquid products were separated by filtration.

2.2.2. Product analysis

Due to the use of water, the liquid products obtained from EHL liquefaction and further upgrading were extracted with dichloromethane (50 mL), and the monomers in dichloromethane were qualitatively and quantitatively analyzed with a Shimadzu GC-MS

(QP2010SE with Optic 4) and an Agilent 7890 GC-FID, respectively. The operating conditions for both GC instruments are described in our previous work [37]. n-Dodecane served as the internal standard for quantification. The total carbon yield of monomers was determined using Eq. (2):

$$\text{Total carbon yield of monomers (\%)} = \sum_i \frac{M(i) \times C(i)}{M(\text{EHL}) \times C(\text{EHL})} \times 100\% \quad (2)$$

Herein, M(i) represents the weight of product i, C(i) represents the weight percentage of carbon in product i, M(EHL) represents the weight of EHL added into the reaction, and C(EHL) represents the weight percentage of carbon in EHL.

The gas sample was collected with a bomb and analysed with a gas chromatography (GC, Agilent Technologies, model 6890) equipped with a flame ionization detector (FID, Column: Al₂O₃/KCl, 50 m × 0.32 mm × 8.0 μm) and a thermal conductivity detector (TCD, Columns: HP-PLOT Q, 30 m × 0.53 mm × 40 μm; MoleSieve 5A, 30 m × 0.53 mm × 25 μm).

The non-volatile products were obtained through the evaporation of solvents and small molecule products through vacuum evaporation at 80 °C. Heteronuclear single quantum coherence nuclear magnetic resonance (HSQC-NMR) spectra of EHL and the non-volatile products were recorded at room temperature on a Bruker AVANCE III HD 400 MHz spectrometer. To ensure the accuracy of semi-quantification regarding the β-O-4 linkage content in both EHL and its products, precise sample quantities (50 mg) and solvent volumes (600 μL DMSO-*d*₆) were meticulously measured and maintained.

The average molecular weight of EHL as well as the non-volatile products was determined using an Agilent HPLC system with Phenogel columns (5 μm – 5 nm and 100 nm) and a UV detector set at 280 nm. Tetrahydrofuran was used as the eluent at a flow rate of 1.0 ml min⁻¹.

2.2.3. Variable-temperature operando HSQC-NMR spectroscopy

Variable-temperature HSQC-NMR spectra of EHL in isopropanol-*d*₈ and the mixture of isopropanol-*d*₈ and D₂O were recorded on a modified Bruker AVANCE III HD 400 MHz spectrometer. The maximum operating temperature is 150 °C. In a typical procedure, 150 mg of EHL and 2 mL of solvent were introduced into a 10 mL quartz high pressure NMR tube. Subsequently, the quartz tube was sealed with 2 MPa N₂ and then heated to 150 °C for 15 min and kept at this temperature for 3 h in the NMR spectrometer prior to measurements.

2.2.4. Molecular dynamics simulations

Molecular dynamics simulations were carried out using the Forcite module in the Materials Studio software. The lignin model was constructed by connecting 20 G units with β-O-4 bonds. Solvent density was set at half of the real liquid density, following experimental conditions. Canonical ensemble simulations (NVT) were performed for 2000 ps at 250 °C for all models, with a time step of 1 fs. The first 1000 ps were utilized for system equilibration, and the subsequent 1000 ps were dedicated to data analysis. The COMPASSII force field was employed to describe intermolecular interactions, and charges were assigned based on the force field. Hydrogen bonding interaction energies were computed using the Ewald method with an accuracy of 0.001 kcal/mol, whereas van der Waals interaction energies were computed using the Atom-based method with a cutoff distance of 15.5 Å. The van der Waals and hydrogen bonding interaction energies between lignin and solvent (E_{vdW}(lignin-solvent) and E_H(lignin-solvent)) were calculated with the Eqs. (3) and (4):

$$E_{\text{vdW}}(\text{lignin-solvent}) = E_{\text{vdW}}(\text{system}) - E_{\text{vdW}}(\text{lignin}) - E_{\text{vdW}}(\text{solvent}) \quad (3)$$

$$E_{\text{H}}(\text{lignin-solvent}) = E_{\text{H}}(\text{system}) - E_{\text{H}}(\text{lignin}) - E_{\text{H}}(\text{solvent}) \quad (4)$$

Here, E_{vdW}(system), E_{vdW}(lignin) and E_{vdW}(solvent) represent the van der Waals interaction energies in the entire system, within lignin molecules,

and between solvent molecules, respectively. Similarly, $E_{H(\text{system})}$, E_H (lignin) and $E_{H(\text{solvent})}$ denote the hydrogen bonding interaction energies in the entire system, within lignin molecules, and between solvent molecules, respectively. These equations employed average values calculated from results obtained between 1000 to 2000 ps.

3. Results

3.1. Non-catalytic EHL solvolysis

The non-catalytic solvolysis of 1 g EHL in 50 mL pure alcohol/alcohol-H₂O mixtures was investigated at 250 °C, see Fig. 1 (a). The liquefaction degree of EHL in pure methanol is 92.6 wt%, higher than that obtained in pure ethanol and isopropanol, which are 88.4 wt% and 67.5 wt%, respectively. Despite the low EHL liquefaction degree in H₂O (<20 wt%), the addition of H₂O into these alcohols increases the EHL liquefaction degree. When the volume ratio of alcohol to H₂O is fixed at 3:2, the mixture of isopropanol and H₂O achieves complete EHL liquefaction, and the liquefaction degrees obtained in ethanol-H₂O and methanol-H₂O are 95.8 and 94.6 wt%, respectively. The effect of the volume ratio of isopropanol to H₂O was examined. The liquefaction degree of EHL obtained in isopropanol-H₂O (2:3) is 97.7 wt%, slightly lower than that obtained in isopropanol-H₂O (3:2). In isopropanol-H₂O with volume ratios of 1:4 and 4:1, the liquefaction degrees of EHL are only 84.9 and 87.3 wt%, respectively. The effects of volume ratios of alcohol to H₂O in methanol-H₂O and ethanol-H₂O mixtures were also examined (Figs. S1 and S2), revealing that methanol-H₂O and ethanol-H₂O mixtures can not achieve a 100 wt% EHL liquefaction degree across different alcohol to H₂O volume ratios. Therefore, isopropanol-H₂O (2:3) is the most efficient solvent for non-catalytic EHL solvolysis, among the solvent examined.

The effect of reaction temperature on the EHL liquefaction degree in isopropanol-H₂O (3:2) and pure isopropanol was investigated (Fig. 1 (b)). At 50 °C, EHL has a higher solubility in isopropanol-H₂O (3:2) compared to pure isopropanol. With increasing the reaction

temperature, the difference in EHL liquefaction degree between isopropanol-H₂O (3:2) and pure isopropanol became more pronounced. The EHL liquefaction degree reaches 100 wt% in isopropanol-H₂O (3:2) at 200 °C, while the value obtained in isopropanol at 200 °C is only 63.7 wt%. At 250 °C, isopropanol-H₂O (3:2) also achieves complete EHL liquefaction, whereas isopropanol only dissolves 67.4 wt% of EHL. The effect of the amount of EHL on its liquefaction degree in 50 mL isopropanol-H₂O (3:2) was examined at 200 and 250 °C (Fig. 1 (c)). At 200 °C, 1.5 g EHL is completely liquefied in 50 mL isopropanol-H₂O (3:2), with the liquefaction degree significantly decreasing as the amount of EHL is further increased. Nevertheless, at 250 °C, isopropanol-H₂O (3:2) achieves complete liquefaction of 2 g EHL, and the EHL liquefaction degree is 90.3 wt% with 3 g EHL.

The monomers in the liquid phase obtained from non-catalytic EHL solvolysis at 250 °C were identified using GC-MS and quantified with GC-FID. As shown in Fig. 2 (a) and (b), the major monomers are *para*-ethyl and vinyl-substituted phenol and guaiacol, and other monomers include ketone-substituted guaiacol and syringol, 4-propenyl syringol, and esters derived from ferulic and *p*-coumaric acids. *Para*-ethyl phenolics are generated through hydrogen transfer from the alcohol to *para*-vinyl side chains.

The mole ratio of *para*-vinyl substituted products to *para*-ethyl substituted products ($n(\text{C}=\text{C}):n(\text{C}-\text{C})$) was employed to assess the hydrogen transfer activity of the solvent, see Fig. 2 (c). This ratio is 0.77 in methanol, and decreases to 0.52 in ethanol. In isopropanol, the ratio is only 0.03, indicating that isopropanol shows much higher hydrogen transfer activity compared to methanol and ethanol. In the non-catalytic solvolysis process, active products are stabilized with alcohol solvent [6]. Isopropanol, with higher hydrogen transfer activity, is more efficient in product stabilization than methanol and ethanol, thereby suppressing condensation reactions [25]. The hydrogen transfer activity are lower for methanol-H₂O (3:2), ethanol-H₂O (3:2), and isopropanol-H₂O (3:2) than those of the corresponding pure alcohols, with the ratio $n(\text{C}=\text{C}):n(\text{C}-\text{C})$ being 0.82, 0.70, and 0.38, respectively. Nevertheless, isopropanol-H₂O (3:2) still exhibits higher hydrogen transfer activity compared to pure methanol, pure ethanol, methanol-H₂O (3:2) and ethanol-H₂O (3:2).

The total carbon yields of monomers obtained in different solvents are also displayed in Fig. 2 (c). The total monomer yields obtained in pure alcohols exhibit an inversely proportional to the $n(\text{C}=\text{C}):n(\text{C}-\text{C})$ ratio. Isopropanol gives the highest total carbon yield of monomers, reaching 6.4 %, among the pure alcohols, whereas ethanol and methanol yield 5.2 and 4.0 % of monomers, respectively. The hydrogenation of $\text{C}=\text{C}$ bonds is believed to suppress condensation reactions, contributing to the high monomer yield [38]. However, the total carbon yields of monomers obtained in alcohol-H₂O mixtures are lower than those obtained in pure alcohols, specifically 2.6, 3.4 and 4.2 % in methanol-H₂O (3:2), ethanol-H₂O (3:2) and isopropanol-H₂O (3:2), respectively. This may be due to certain monomers not being effectively extracted from alcohol-H₂O mixtures into dichloromethane.

Fig. 3 (a, b and c) displays the HSQC-NMR spectra of EHL and the liquid products obtained in pure isopropanol and isopropanol-H₂O (3:2) at 250 °C. In the spectrum of original EHL, signals corresponding to $\text{C}\alpha$ - $\text{H}\alpha$, $\text{C}\beta$ - $\text{H}\beta$, and $\text{C}\gamma$ - $\text{H}\gamma$ in β -O-4 linkage (labeled as $\text{A}\alpha$, $\text{A}\beta$, and $\text{A}\gamma$) are identified. Due to the significantly stronger intensity of $\text{A}\gamma$ signal compared to $\text{A}\alpha$ and $\text{A}\beta$ signals, $\text{A}\gamma$ signal was used for semi-quantification of the β -O-4 linkage content in EHL and products. DMSO-*d*₆ solvent was chosen as the internal standard because the ratio between the signals of $\text{A}\gamma$ and DMSO-*d*₆ remains consistent within the same sample across different NMR runs, and its intensity and position are also unaffected by the reaction as it is added after the reaction [37]. The signal of $\text{A}\gamma$ were normalized with respect to the peak of the DMSO-*d*₆ solvent. The relative intensity (RI) of $\text{A}\gamma$ in the spectrum of the original EHL is 1.33, while this value is reduced to 0.82 after reaction in isopropanol and further decreases to 0.69 after reaction in isopropanol-H₂O (3:2). The weight-average molecular weight (M_w) of the original

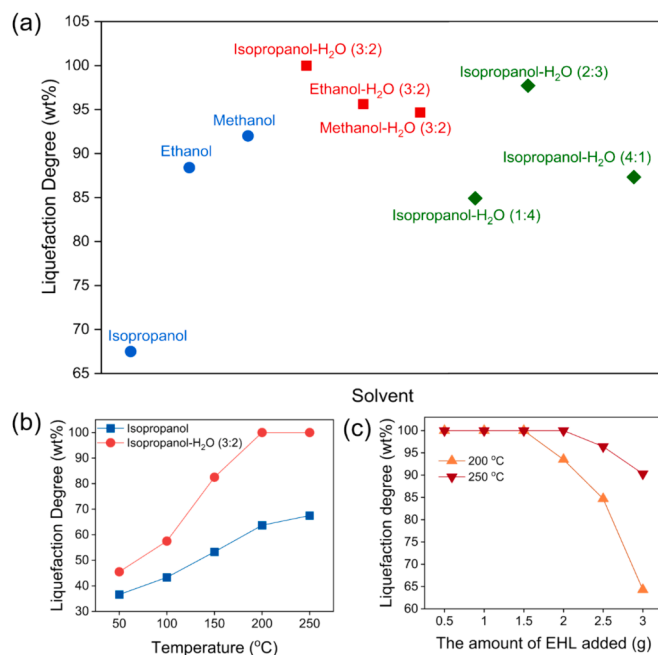


Fig. 1. (a) Liquefaction degree of 1 g EHL in 50 mL solvent at 250 °C for 3 h under a N₂ atmosphere. (b) Liquefaction degree of 1 g EHL in 50 mL isopropanol and isopropanol-H₂O (3:2) for 3 h under a N₂ atmosphere at different reaction temperatures. (c) EHL liquefaction degree in 50 mL isopropanol-H₂O (3:2) with different amounts of EHL added at 200 and 250 °C for 3 h under a N₂ atmosphere.

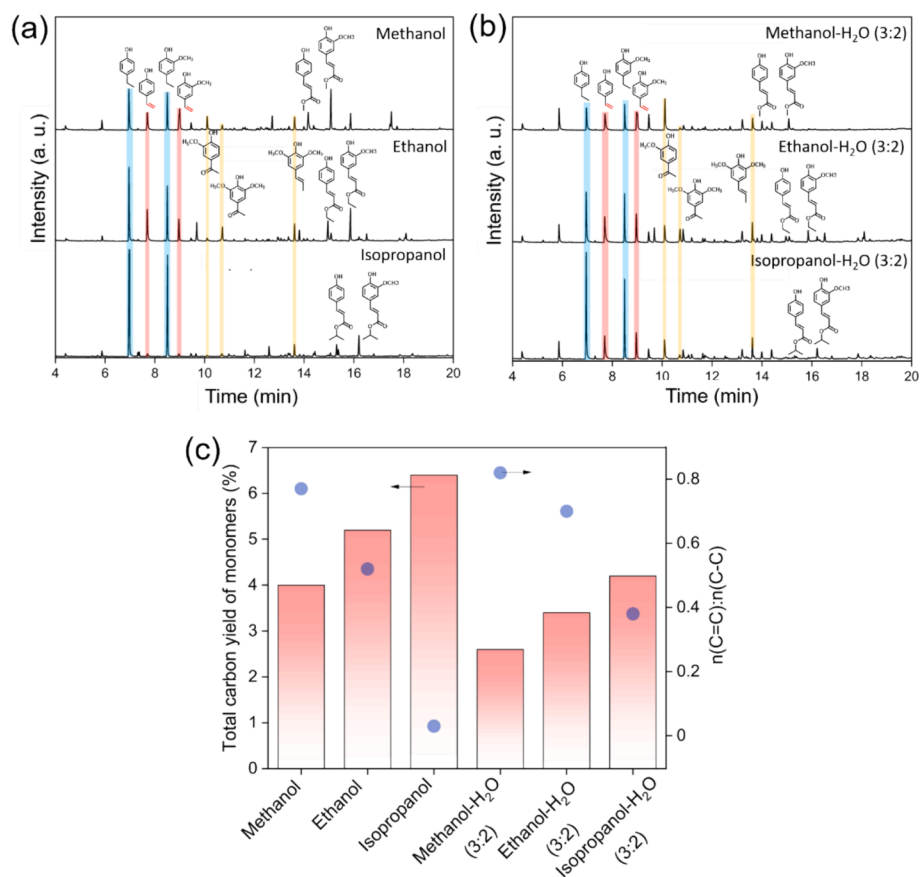


Fig. 2. (a) GC-FID chromatograms and monomer structures detected in pure alcohols. (b) GC-FID chromatograms and monomer structures detected in alcohol-H₂O mixtures. (c) Total carbon yield of monomers and the n(C=C)/n(C-C) ratio obtained in non-catalytic EHL solvolysis (reaction conditions: 1 g EHL, 50 mL solvent, 250 °C, 3 h, N₂ atmosphere).

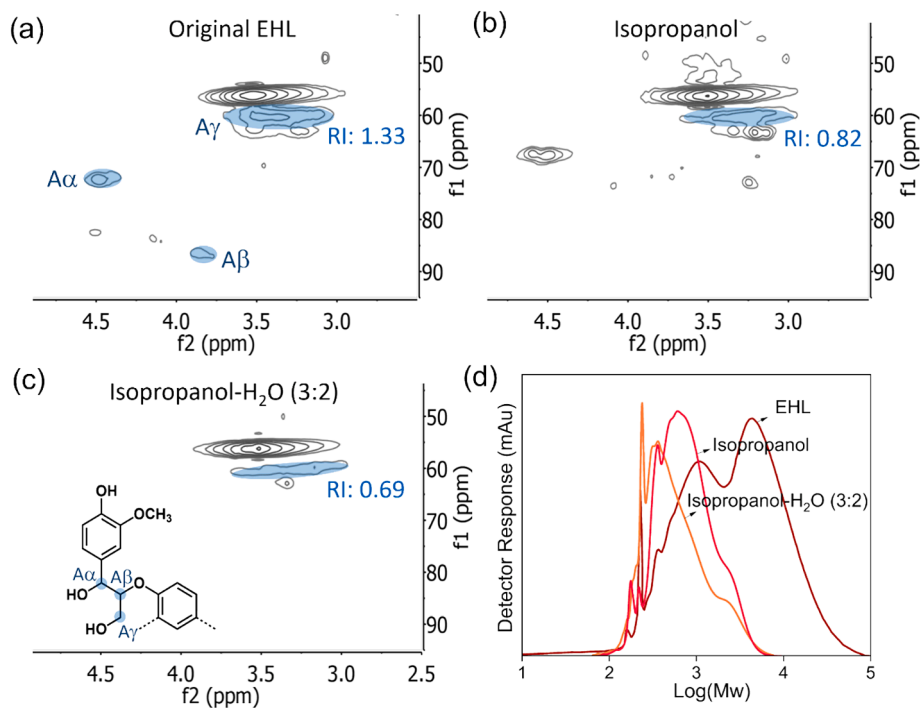


Fig. 3. HSQC-NMR spectra of original EHL (a) and liquid products obtained in pure isopropanol (b) and isopropanol-H₂O (3:2) (c) and their molecular weight distribution (d). (Reaction conditions: 1 g EHL, 50 mL solvent, 250 °C, 3 h, N₂ atmosphere).

EHL and the liquid products was analyzed with GPC (Fig. 3 (d)). The Mw of the liquid product obtained in isopropanol is 894 g/mol, significantly lower than that of the original EHL (4333 g/mol), and further decreases to 759 g/mol in isopropanol-H₂O (3:2). These results indicate that EHL undergoes partial depolymerization during non-catalytic solvolysis in isopropanol at 250 °C, and the addition of H₂O into isopropanol promotes EHL depolymerization.

3.2. Interactions between EHL and solvent

The interactions between EHL and isopropanol or isopropanol-H₂O (3:2) was investigated using variable-temperature operando HSQC-NMR spectroscopy. The spectra of EHL in isopropanol-d₈ and a mixture of isopropanol-d₈ and D₂O (isopropanol-d₈-D₂O (3:2)) acquired at 150 °C are presented in Fig. 4. Three prominent signals were analyzed, i.e. those corresponding to the methoxy groups (-OCH₃), C α -H α in β -O-4 linkages (A α) and C5-H5 in the aromatic rings of G units (G5). Compared to isopropanol-d₈, the -OCH₃ signals in isopropanol-d₈-D₂O (3:2) shifts to a lower field (higher δ value), changing from δ H/ δ C 3.76/56.66 ppm to 3.86/57.27 ppm. Similarly, the A α signal also shifts to a lower field, changing from δ H/ δ C 4.90/73.45 ppm in isopropanol-d₈ to 4.98/73.80 ppm in isopropanol-d₈-D₂O (3:2). These shifts suggest the formation of stronger hydrogen bonds between EHL and isopropanol-d₈-D₂O (3:2) than that between EHL and isopropanol alone, which results in a more pronounced effect on reducing the electron density of these groups [39–41]. In addition, the signal G5 in isopropanol-d₈-D₂O (3:2) is shifted to a higher field compared to that in isopropanol-d₈, changing from δ H/ δ C 6.85/116.38 ppm to 6.74/116.32 ppm. This shift may be attributed to the disruption of π - π stacking interactions between the aromatic rings in EHL by the solvent [42–44].

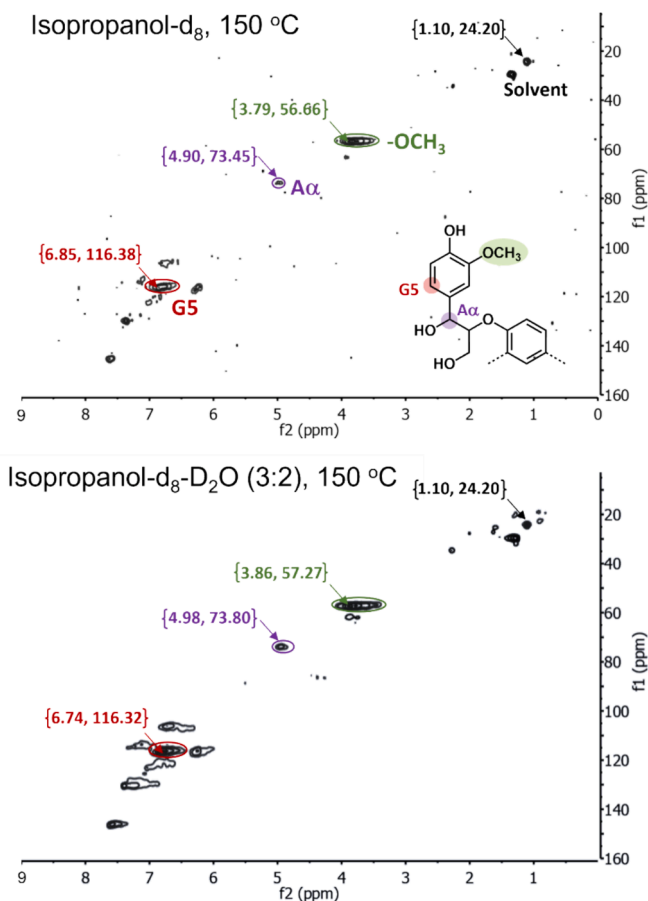


Fig. 4. Operando HSQC-NMR spectra of EHL in isopropanol-d₈ and isopropanol-d₈-D₂O (3:2) at 150 °C.

The structural configurations of a large lignin fragment, containing 20 aromatic rings, after a 2000 ps molecular dynamics simulations in the different solvents are shown in Fig. 5 (a). In H₂O, the lignin is considerably aggregated, whereas, in isopropanol, it disassembles to some extent, and, in isopropanol-H₂O (3:2), the lignin fragment is significant open and stretched. Interestingly, despite extensive lignin aggregation in H₂O, H₂O exhibits a lower interaction energy with the lignin compared to isopropanol, indicating a stronger interaction between the lignin and H₂O (Fig. 5 (b)). The interactions between H₂O and lignin comprise mainly hydrogen bonds, accounting for 83 % of the total interaction energy between lignin and H₂O. In contrast, in isopropanol, the hydrogen bonding and van der Waals interaction energies are comparable, i.e., 41 % and 59 %, respectively, indicating that both types of interactions play a role in EHL solubilization. Compared to pure H₂O and pure isopropanol, the isopropanol-H₂O (3:2) mixture has a lower total interaction energy and more balanced proportion of hydrogen bonding (47 %) and van der Waals (53 %) interaction energies with lignin. Hence, the EHL liquefaction degree in isopropanol-H₂O (3:2) is higher than those in pure H₂O and isopropanol.

The solvent distribution around the functional groups in lignin was evaluated using radial distribution function (RDF) analysis to provide more detailed information about the interaction between lignin and the solvents [45–47]. In Fig. 5 (c1–c3) and (d1–d3), $g(r)$ represents the relative density of solvent atoms (H or O) in a spherical area centered on a lignin atom, and r denotes the radius of the spherical area. Fig. 5 (c1) shows the results of the RDF analysis of H atoms in solvents surrounding O atoms in the hydroxyl groups of lignin. For H₂O, isopropanol and isopropanol-H₂O (3:2), a peak at 1.9 Å is observed, corresponding to the formation of solvent shells attributed to hydrogen bond interactions between the solvents and the hydroxyl groups present in lignin [48]. Nevertheless, the $g(r)$ value at 1.9 Å of H₂O is higher than that of isopropanol-H₂O (3:2) and isopropanol, indicating that H₂O, as a solvent, more readily approaches the hydroxyl groups. In the $g(r)$ curves of the H atoms in the solvents around the O atoms in the ether bonds of lignin (Fig. 5 (c2)), only H₂O exhibits a weak peak at 2 Å, while isopropanol-H₂O (3:2) and isopropanol do not have an obvious peak. This indicates that the formation of hydrogen bonds between the solvents and ether bonds of lignin is more difficult than that with hydroxyls of lignin. Nevertheless, beyond 2.5 Å, the $g(r)$ value of H₂O is notably lower than that of the other two solvents, which may be attributed to hindrance caused by hydrophobic groups, such as aliphatic chains and aromatic rings around the ether bonds, impeding the approach of H₂O [46]. The hydrophobic effect is notably pronounced in the $g(r)$ curves of O atoms in solvents around the carbon atoms in the aromatic rings of lignin (Fig. 5 (c3)). In this curve, all $g(r)$ values of the solvents are nearly 0 when r is below 2.5 Å, indicating the absence of hydrogen bonds between the solvents and the aromatic rings in lignin [49]. As the value of r extends to the range of van der Waals forces, specifically from 2.5 to 5 Å, the $g(r)$ of isopropanol-H₂O (3:2) is slightly higher than that of pure isopropanol, and significantly higher than that of pure H₂O, indicating that the solvent mixture more readily approaches the aromatic rings.

In order to elucidate the role of H₂O and isopropanol in the isopropanol-H₂O (3:2) mixture, the RDF of H₂O and isopropanol in isopropanol-H₂O (3:2) around the functional groups in lignin were analyzed separately, see Fig. 5 (d1–d3). Around the hydroxyl groups of lignin, the $g(r)$ value of the H atoms in H₂O is much higher than that of isopropanol, and two peaks at 1.9 and 3.2 Å appear in the $g(r)$ curve of H₂O (Fig. 5 (d1)). Hence, H₂O is primarily responsible for forming hydrogen bonds with the hydroxyl groups of lignin in the mixture solvent. In addition, H₂O may approach ether bonds in lignin more easily than isopropanol (Fig. 5 (d2)). In contrast to the curves in Fig. 5 (c2), the $g(r)$ value of the H atoms in H₂O consistently exceeds that in isopropanol within the range 1 to 5 Å. This suggests a synergistic effect between H₂O and isopropanol, facilitating the approach of H₂O to ether bonds in lignin. Nevertheless, around the aromatic rings of lignin, the $g(r)$ value of the O atom in isopropanol is much higher than that of O in H₂O (Fig. 5

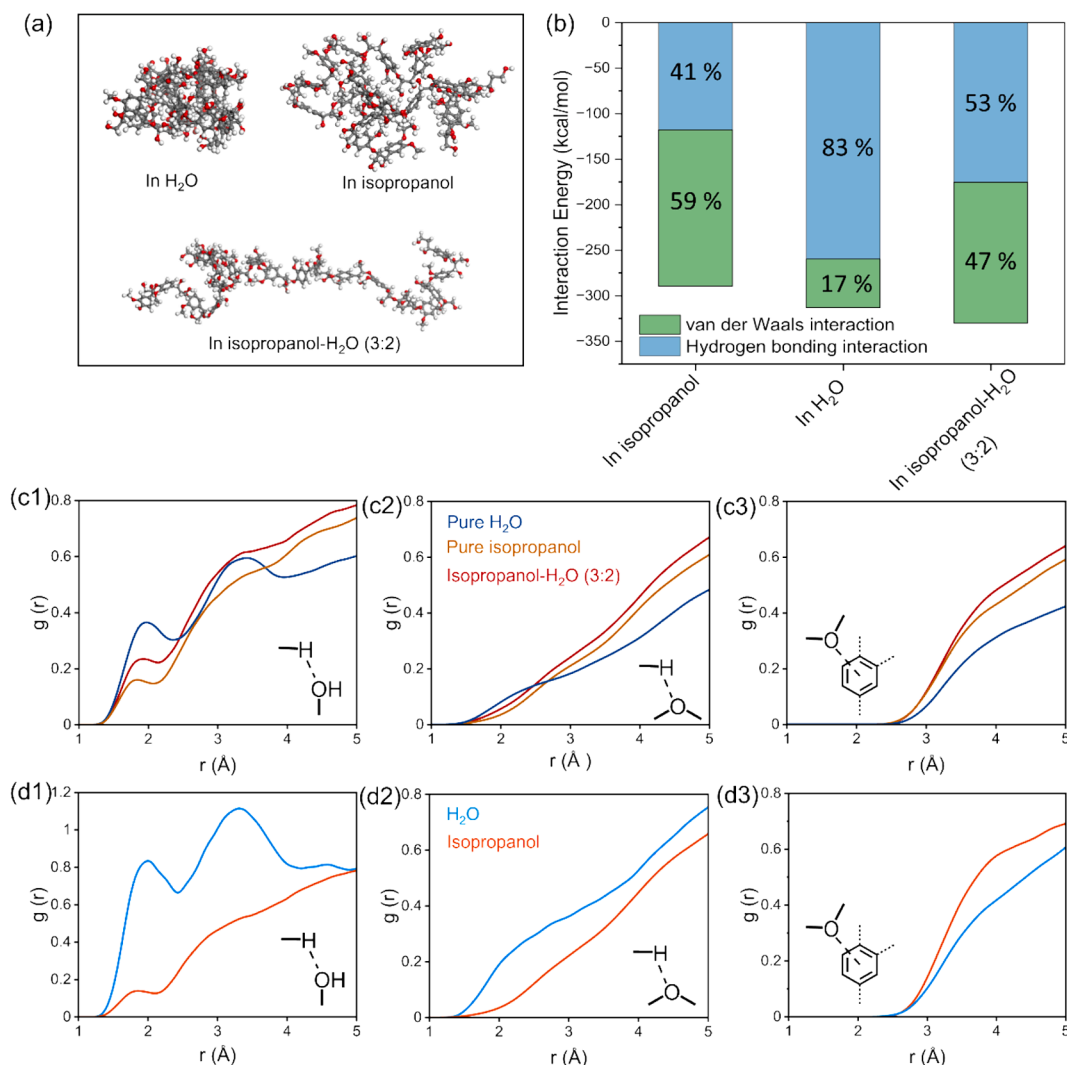


Fig. 5. (a) Optimized structural configurations of a lignin fragment in water, isopropanol and isopropanol-H₂O (3:2), (b) Total interaction energy between lignin and solvent, (c1-c3) the RDF analysis of solvents around the functional groups in lignin, (d1-d3) the RDF of H₂O and isopropanol in isopropanol-H₂O (3:2) around the functional groups in lignin.

(d3)), indicating that isopropanol preferentially interacts with the aromatic rings through van der Waals forces compared to water.

3.3. Product upgrading

The liquid product obtained from the solvolysis of 1 g EHL in 50 mL isopropanol-H₂O (3:2) at 250 °C was further upgraded using Raney Ni at 320 °C under a N₂ atmosphere. In the upgrading process, large lignin fragments in the liquid product undergo depolymerization, and monomers and oligomers undergo further HDO reactions. Simultaneously, the isopropanol-H₂O reforming reaction takes place, providing hydrogen for both the depolymerization and HDO reactions. The monomer products identified in product upgrading are illustrated in Fig. 6 (a). The total carbon yield of identified monomers is 45.6 %, with a selectivity of 35.1 % for cycloalkanes (cyclohexane, methylcyclohexane ethylcyclohexane and propylcyclohexane), 51.6 % for arenes (benzene, toluene, ethylbenzene and propylbenzene), and 13.3 % for alkylphenols (phenol, methylphenol, ethylphenol, and propylphenol).

Gas products were also quantified as depicted in Fig. 6 (b). In the reaction with only solvent, gaseous products, including H₂ (34.3 mmol), CH₄ (2.7 mmol) and CO₂ (0.6 mmol), were generated through isopropanol-H₂O reforming reactions. In the reaction of EHL product upgrading, the amount of H₂ decreases to 26.9 mmol, indicating that the

hydrogen produced is consumed by product upgrading process. Meanwhile, the amounts of CH₄ and CO₂ increase to 12.4 and 4.6 mmol, respectively, which are attributed to the demethoxylation and decarboxylation of EHL in HDO process.

Non-volatile oligomers, constituting 20.1 wt% of the initial EHL weight, were obtained through the evaporation of solvents and small-molecule products. Although these oligomers can not be identified with GC-MS, their structures and molecular weights were analyzed using HSQC-NMR (Fig. 6 (c)) and GPC (Fig. 6 (d)), respectively. In the HSQC-NMR spectrum of products after upgrading, the signals of β-O-4 linkage (Ay) and S units disappear, and the signals of -OCH₃ and G units are significantly weakened, while the signals of aliphatic C-C bonds and H units are obviously enhanced, compared to the spectrum of products before upgrading. This indicates that the oligomers primarily consist of H units connected with C-C linkages, with the removal of most -OCH₃ groups. In the GPC curve, distinct peaks emerge at Mw values of 240 and 380 mol/g, corresponding to a dimer and a trimer, respectively. The structures of the dimer and trimer were speculated based on their Mw values and HSQC-NMR results, where the dimer contains two phenol units connected with a C-C linkage, and the trimer comprises three phenol units with C-C linkages.

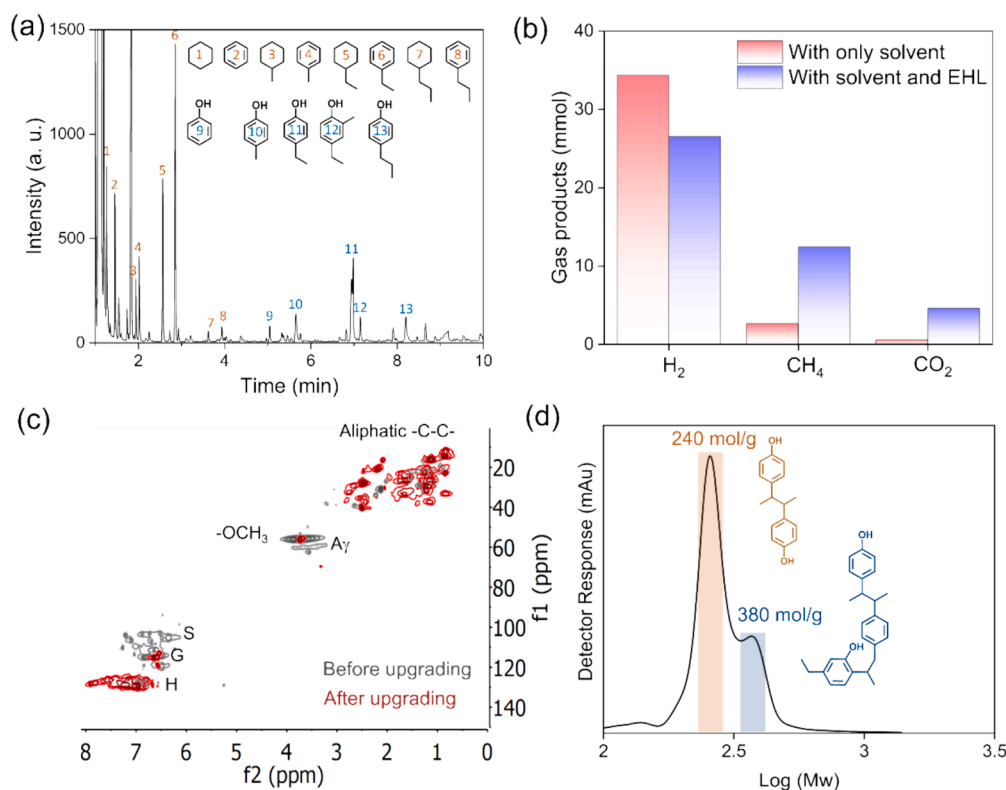


Fig. 6. (a) the GC-FID chromatogram with monomer structures detected after catalytic upgrading. (b) the gas products of the reaction with only solvent and the reaction of EHL product upgrading. (c) the HSQC-NMR spectra of non-volatile products before and after catalytic upgrading. (d) the molecular weight distribution of non-volatile products after catalytic upgrading. (Reaction conditions: 0.5 g Raney Ni, 320 °C, 6 h, N₂ atmosphere.).

4. Discussion

4.1. The advantages of isopropanol-H₂O (3:2) solvent

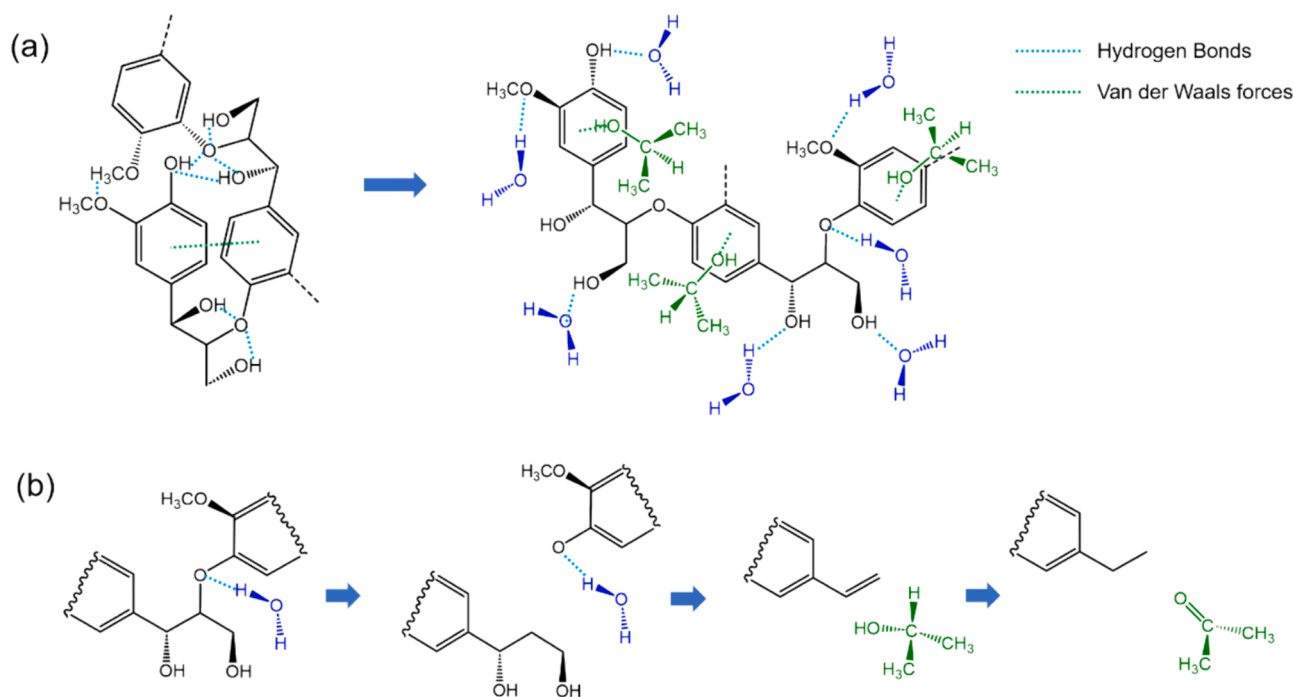
The use of isopropanol-H₂O (3:2) solvent offers two significant advantages for biofuel production from EHL. Firstly, isopropanol-H₂O solvent exhibits a high EHL solubility and achieves complete EHL liquefaction even in the absence of a catalyst at elevated temperatures. EHL solvolysis and product upgrading have mostly been carried out as a batch process, but, with isopropanol-H₂O (3:2) as a solvent, a more efficient continuous flow process could be developed [50]. Ionic liquids (ILs) are reported to be effective solvents for EHL dissolution and liquefaction, but their widespread application is limited by high costs and toxicity concerns [51,52]. In contrast, isopropanol-H₂O (3:2) offers a more cost-effective and environmentally friendly alternative. Additionally, we recently discovered that EHL has a high solubility in ethylene glycol [37]. However, compared to ethylene glycol, isopropanol-H₂O proves to be a more suitable solvent for product separation and upgrading processes due to its lower viscosity and boiling point. Secondly, the use of isopropanol-H₂O (3:2) solvent eliminates the need for additional hydrogen gas in upgrading process. With the isopropanol-H₂O reforming reaction providing the hydrogen, large lignin fragments are further depolymerized and small molecules undergo HDO reaction, resulting in the formation of high amounts of cycloalkanes and arenes. This process represents a more advanced approach compared to using alkanes as solvents, where high pressures of H₂ are required for the formation of cycloalkanes and aromatics in lignin solvolysis and lignin-oil upgrading [53,54].

4.2. The roles of isopropanol and H₂O in EHL liquefaction

EHL has an aggregated structure involving hydrogen bonds between the hydroxyl groups and π - π stacking (van der Waals interaction)

between the aromatic rings [40,55]. In the EHL-solvent mixture, the balanced proportion of hydrogen bonding and van der Waals interaction energies between EHL and the solvent is crucial as it enables the disruption of both hydrogen bonds and π - π stacking in the EHL, facilitating its disaggregation and stretching [41–44,56–59]. H₂O forms strong hydrogen bonds with the hydroxyl groups of EHL but cannot interact with aromatic rings through van der Waals forces. Hence, H₂O alone cannot adequately stretch the aggregated EHL molecules, leading to condensation reactions and char formation during solvolysis. Pure isopropanol interacts with EHL through hydrogen bonding and van der Waals interactions, but the strength of these interactions is insufficient to achieve complete disaggregation and stretching of EHL molecules. Consequently, complete liquefaction of EHL is not achieved in pure isopropanol. Isopropanol-H₂O (3:2) exhibits stronger interactions and a more balanced proportion of hydrogen bonding and van der Waals interaction energies with EHL, compared to pure isopropanol and H₂O. In this mixture, intramolecular interactions within EHL are efficiently disrupted, leading to the effective disaggregation and stretching of EHL molecules. Therefore, isopropanol-H₂O (3:2) achieves complete EHL liquefaction.

In the isopropanol-H₂O (3:2) mixture, a synergistic effect between H₂O and isopropanol promotes the stretching of EHL. As shown in Scheme 1 (a), H₂O disrupts the intra- and inter-molecular hydrogen bonds in EHL, and isopropanol molecules break π - π stacking between aromatic rings by van der Waals forces, facilitating the approach of H₂O to the ether bonds of EHL. The hydrogen bonds between H₂O and the ether bonds in EHL enhance EHL depolymerization, but the initial products from EHL depolymerization are highly active, and easily undergo condensation reactions. Isopropanol stabilizes these active products via hydrogen transfer reaction, thereby suppressing condensation reactions. (Scheme 1 (b)). These combined effects result in complete EHL liquefaction in the absence of a catalyst in the isopropanol-H₂O (3:2) mixture.



Scheme 1. Proposed EHL solvolysis mechanism, including dissolution (a) and depolymerization (b) steps, in a mixture of H₂O and isopropanol.

4.3. Products of upgrading step

The carbon balance of EHL product upgrading is illustrated in Scheme 2. EHL has a carbon content of 61.29%. After the reaction, 45.6% of carbon in EHL is converted into monomers, including 16.0% into cycloalkanes, 23.5% into arenes, and 6.1% into alkylphenols, and 27.1% of carbon in EHL is transformed into gas products, with 19.2% into CH₄ and 7.9% into CO₂, and the remaining 27.3% of carbon in EHL is converted into oligomers. Cycloalkanes and arenes, with a carbon number in the range of C₆-C₉, are well-suited as additives for gasoline. The alkylphenols detected in the product exhibit no methoxy groups, making them suitable feedstocks for phenol-formaldehyde resin production. Gas products rich in CH₄ can be efficiently burned to recover energy. Although the structures of oligomers cannot be accurately determined, the oligomers are inferred to contain 2–3 aromatic rings and have undergone extensive deoxygenation. These oligomers can be further upgraded through cleavage of C-C linkages or directly burned to recover energy [54]. Overall, the product upgrading step achieves efficient depolymerization of large lignin fragment and HDO of small monomers and oligomers.

5. Conclusions

The EHL liquefaction via non-catalytic solvolysis in pure alcohols

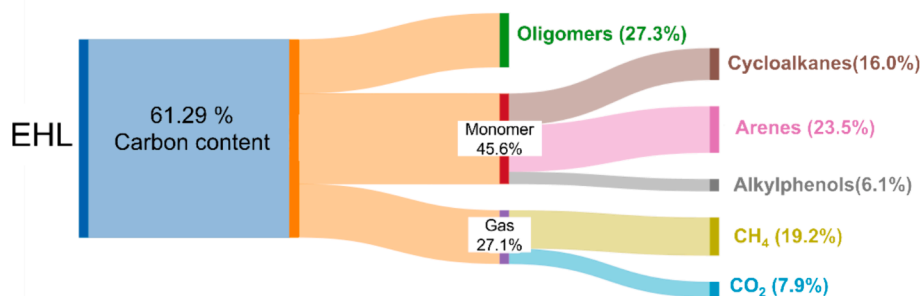
(methanol, ethanol, and isopropanol) and their mixtures with H₂O was investigated. The addition of H₂O into alcohols enhances EHL liquefaction, and isopropanol-H₂O (3:2) demonstrates the highest liquefaction degree, among both pure alcohols and alcohol-H₂O mixtures. In isopropanol-H₂O (3:2), 2 g of EHL was completely liquefied in 50 mL solvent at 250 °C without char formation.

The roles of isopropanol and H₂O in EHL liquefaction involving their interactions with EHL at a molecular level were investigated. In isopropanol-H₂O (3:2), H₂O disrupts the intra- and inter-molecular hydrogen bonds in EHL, and isopropanol breaks π - π stacking interactions between benzene rings in EHL. Additionally, H₂O enhances EHL depolymerization, and isopropanol acts as a hydrogen donor solvent, leading to the stabilization of active intermediates.

The resulting liquid phase products underwent further upgrading in the presence of Raney Ni at 320 °C, with isopropanol-H₂O reforming providing active hydrogens. After the reaction, lignin fragments in the liquid product were further depolymerized, and the resulting lignin monomers underwent HDO reactions, yielding 45.6% of monomers, including cycloalkanes, arenes and alkylphenols.

CRediT authorship contribution statement

Yushuai Sang: Writing – original draft, Investigation, Data curation, Conceptualization. **Gen Li:** Writing – original draft, Software,



Scheme 2. The carbon balance of catalytic upgrading process.

Investigation, Formal analysis. **Xiang Li**: Writing – original draft, Investigation, Data curation, Conceptualization. **Hanzhang Gong**: Writing – original draft, Investigation. **Mingze Yang**: Investigation. **David Savary**: Methodology, Investigation. **Zhaofu Fei**: Methodology, Investigation. **Paul J. Dyson**: . **Hong Chen**: Writing – original draft, Resources, Methodology. **Yongdan Li**: Writing – review & editing, Supervision, Resources, Project administration, Conceptualization.

Declaration of competing interest

The authors declare that they have no known competing financial interests or personal relationships that could have appeared to influence the work reported in this paper.

Data availability

Data will be made available on request.

Acknowledgments

This work was funded by the European Union's Horizon 2020 research and innovation program, (BUILDING A LOW-CARBON, CLIMATE RESILIENT FUTURE: SECURE, CLEAN AND EFFICIENT ENERGY) under Grant Agreement No 101006744. The content presented in this document represents the views of the authors, and the European Commission has no liability in respect of the content.

Appendix A. Supplementary data

Supplementary data to this article can be found online at <https://doi.org/10.1016/j.cej.2024.153624>.

References

- C. Li, X. Zhao, A. Wang, G.W. Huber, T. Zhang, Catalytic Transformation of Lignin for the Production of Chemicals and Fuels, *Chem. Rev.* 115 (2015) 11559–11624.
- Z. Sun, B. Fridrich, A. de Santi, S. Elangovan, K. Barta, Bright Side of Lignin Depolymerization: Toward New Platform Chemicals, *Chem. Rev.* 118 (2018) 614–678.
- N. Sarkar, S.K. Ghosh, S. Bannerjee, K. Aikat, Bioethanol production from agricultural wastes: an overview, *Renew. Energ.* 37 (2012) 19–27.
- M. Balat, H. Balat, Recent trends in global production and utilization of bio-ethanol fuel, *Appl. Energy* 86 (2009) 2273–2282.
- D.S. Bajwa, G. Pourhashem, A.H. Ullah, S.G. Bajwa, A concise review of current lignin production, applications, products and their environmental impact, *Ind. Crop. Prod.* 139 (2019).
- Y. Sang, H. Chen, M. Khalifeh, Y. Li, Catalysis and chemistry of lignin depolymerization in alcohol solvents-A review, *Catal. Today* 408 (2023) 168–181.
- V. Patil, S. Adhikari, P. Cross, H. Jahromi, Progress in the solvent depolymerization of lignin, *Renew. Sust. Energ. Rev.* 133 (2020).
- L. Shuai, J. Luterbacher, Organic Solvent Effects in Biomass Conversion Reactions, *ChemSusChem* 9 (2016) 133–155.
- K. Zhang, Z. Pei, D. Wang, Organic solvent pretreatment of lignocellulosic biomass for biofuels and biochemicals: A review, *Bioresour. Technol.* 199 (2016) 21–33.
- D. Raikwar, S. Majumdar, D. Shee, Effects of solvents in the depolymerization of lignin into value-added products: a review, *Biomass Convers. Biorefin.* (2021).
- K. Wu, S. Kasipandi, Z. Wen, F. Yan, Y. Sang, Z. Ma, M. Chen, H. Chen, Y. Li, Selective demethoxylation of guaiacol to alkylphenols in supercritical methanol over a HT-MoS₂ catalyst, *Catal. Today*, 2020.
- K. Wu, Y. Sang, S. Kasipandi, Y. Ma, H. Jiao, Q. Liu, H. Chen, Y. Li, Catalytic roles of Mo-based sites on MoS₂ for ethanolysis of enzymatic hydrolysis lignin into aromatic monomers, *Catal. Today* 408 (2023) 211–222.
- Y. Sang, M. Chen, F. Yan, K. Wu, Y. Bai, Q. Liu, H. Chen, Y. Li, Catalytic depolymerization of enzymatic hydrolysis lignin into monomers over an unsupported nickel catalyst in supercritical ethanol, *Ind. Eng. Chem. Res.* 59 (2020) 7466–7474.
- Y. Bai, K. Cui, Y. Sang, K. Wu, F. Yan, F. Mai, Z. Ma, Z. Wen, H. Chen, M. Chen, Y. Li, Catalytic Depolymerization of a Lignin-Rich Corn Cob Residue into Aromatics in Supercritical Ethanol over an Alumina-Supported NiMo Alloy Catalyst, *Energy Fuels* 33 (2019) 8657–8665.
- F. Mai, Z. Wen, Y. Bai, Z. Ma, K. Cui, K. Wu, F. Yan, H. Chen, Y. Li, Selective conversion of enzymatic hydrolysis lignin into alkylphenols in supercritical ethanol over a WO₃/γ-Al₂O₃ catalyst, *Ind. Eng. Chem. Res.* 58 (2019) 10255–10263.
- C. Cheng, D. Shen, S. Gu, K.H. Luo, State-of-the-art catalytic hydrogenolysis of lignin for the production of aromatic chemicals, *Catal. Sci. Technol.* 8 (2018) 6275–6296.
- M.J. Gilkey, B. Xu, Heterogeneous Catalytic Transfer Hydrogenation as an Effective Pathway in Biomass Upgrading, *ACS Catal.* 6 (2016) 1420–1436.
- Y. Jing, L. Dong, Y. Guo, X. Liu, Y. Wang, Chemicals from Lignin: A Review of Catalytic Conversion Involving Hydrogen, *ChemSusChem* (2020).
- S. Cheng, C. Wilks, Z. Yuan, M. Leitch, C. Xu, Hydrothermal degradation of alkali lignin to bio-phenolic compounds in sub/supercritical ethanol and water-ethanol co-solvent, *Polym. Degrad. and Stabil.* 97 (2012) 839–848.
- J.-Y. Kim, S. Oh, H. Hwang, T.-S. Cho, I.-G. Choi, J.W. Choi, Effects of various reaction parameters on solvolytic depolymerization of lignin in sub- and supercritical ethanol, *Chemosphere* 93 (2013) 1755–1764.
- K.H. Kim, R.C. Brown, M. Kieffer, X. Bai, Hydrogen-donor-assisted solvent liquefaction of lignin to short-chain alkylphenols using a micro reactor/gas chromatography system, *Energy Fuels* 28 (2014) 6429–6437.
- D. Guo, B. Liu, Y. Tang, J. Zhang, X. Xia, Autocatalytic Depolymerization of Alkali Lignin by Organic Bound Sodium in Supercritical Ethanol, *Energy Fuels* 31 (2017) 10842–10849.
- J.B. Nielsen, A. Jensen, L.R. Madsen, F.H. Larsen, C. Felby, A.D. Jensen, Noncatalytic Direct Liquefaction of Biorefinery Lignin by Ethanol, *Energy Fuels* 31 (2017) 7223–7233.
- J.B. Nielsen, A. Jensen, C.B. Schandel, C. Felby, A.D. Jensen, Solvent consumption in non-catalytic alcohol solvolysis of biorefinery lignin, *Sustain. Energy Fuels* 1 (2017) 2006–2015.
- C. Cheng, J. Truong, J.A. Barrett, D. Shen, M.M. Abu-Omar, P.C. Ford, Hydrogenolysis of Organosolv Lignin in Ethanol/Isopropanol Media without Added Transition-Metal Catalyst, *ACS Sustainable Chem. Eng.* 8 (2019) 1023–1030.
- P.D. Kouris, D.J.G.P. van Osch, G.J.W. Creemers, M.D. Boot, E.J.M. Hensen, Mild thermolytic solvolysis of technical lignins in polar organic solvents to a crude lignin oil, *Sustain. Energy Fuels* 4 (2020) 6212–6226.
- X. Kong, C. Liu, Y. Fan, M. Li, R. Xiao, Depolymerization of technical lignin to valuable platform aromatics in lower alcohol without added catalyst and external hydrogen, *Fuel Process. Technol.* 242 (2023) 107637.
- S. Kim, E.E. Kwon, Y.T. Kim, S. Jung, H.J. Kim, G.W. Huber, J. Lee, Recent advances in hydrodeoxygenation of biomass-derived oxygenates over heterogeneous catalysts, *Green Chem.* 21 (2019) 3715–3743.
- J.H. Zhang, J.M. Sun, Y. Wang, Recent advances in the selective catalytic hydrodeoxygenation of lignin-derived oxygenates to arenes, *Green Chem.* 22 (2020) 1072–1098.
- H. Wei, Z. Wang, H.J.G.C. Li, Sustainable biomass hydrodeoxygenation in biphasic systems, *Green Chem.* 24 (2022) 1930–1950.
- Q. Xia, Z. Chen, Y. Shao, X. Gong, H. Wang, X. Liu, S.F. Parker, X. Han, S. Yang, Y. Wang, Direct hydrodeoxygenation of raw woody biomass into liquid alkanes, *Nat. Commun.* 7 (2016) 1–10.
- L. Dong, L. Lin, X. Han, X. Si, X. Liu, Y. Guo, F. Lu, S. Rudić, S.F. Parker, S. Yang, Y. Wang, Breaking the Limit of Lignin Monomer Production via Cleavage of Interunit Carbon-Carbon Linkages, *Chem* 5 (2019) 1521–1536.
- Y. Guo, Y. Jing, Q. Xia, Y. Wang, NbOx-Based Catalysts for the Activation of C-O and C-C Bonds in the Valorization of Waste Carbon Resources, *Acc. Chem. Res.* 55 (2022) 1301–1312.
- T. Ren, S. You, M. Zhang, Y. Wang, W. Qi, R. Su, Z. He, Improved conversion efficiency of Lignin-to-Fuel conversion by limiting catalyst deactivation, *Chem. Eng. J.* 410 (2021) 128270.
- P. Sun, Z. Wang, C. Li, B. Tang, C. Peng, Catalytic conversion of lignin and its derivatives to alkanes over multifunctional catalysts: A review, *Fuel* 361 (2024) 130726.
- Y. Sang, K. Wu, Q. Liu, Y. Bai, H. Chen, Y. Li, Catalytic ethanolysis of enzymatic hydrolysis lignin over an unsupported nickel catalyst: the effect of reaction conditions, *Energy Fuels* 35 (2020) 519–528.
- Y. Sang, Y. Ma, G. Li, K. Cui, M. Yang, H. Chen, Y. Li, Enzymatic hydrolysis lignin dissolution and low-temperature solvolysis in ethylene glycol, *Chem. Eng. J.* 463 (2023) 142256.
- Y.M. Questell-Santiago, M.V. Galkin, K. Barta, J.S. Luterbacher, Stabilization strategies in biomass depolymerization using chemical functionalization, *Nat. Rev. Chem* 4 (2020) 311–330.
- J. Sun, T. Dutta, R. Parthasarathi, K.H. Kim, N. Tolic, R.K. Chu, N.G. Isern, J. R. Cort, B.A. Simmons, S. Singh, Rapid room temperature solubilization and depolymerization of polymeric lignin at high loadings, *Green Chem.* 18 (2016) 6012–6020.
- C. Crestini, H. Lange, M. Sette, D.S. Argyropoulos, On the structure of softwood kraft lignin, *Green Chem.* 19 (2017) 4104–4121.
- A. Xu, X. Guo, Y. Zhang, Z. Li, J. Wang, Efficient and sustainable solvents for lignin dissolution: aqueous choline carboxylate solutions, *Green Chem.* 19 (2017) 4067–4073.
- Y. Zhang, H. He, K. Dong, M. Fan, S. Zhang, A DFT study on lignin dissolution in imidazolium-based ionic liquids, *RSC Adv.* 7 (2017) 12670–12681.
- H. Ji, P. Lv, Mechanistic insights into the lignin dissolution behaviors of a recyclable acid hydrotrope, deep eutectic solvent (DES), and ionic liquid (IL), *Green Chem.* 22 (2020) 1378–1387.
- L. Chen, S.-M. Luo, C.-M. Huo, Y.-F. Shi, J. Feng, J.-Y. Zhu, W. Xue, X. Qiu, New insight into lignin aggregation guiding efficient synthesis and functionalization of a lignin nanosphere with excellent performance, *Green Chem.* 24 (2022) 285–294.
- L. Petridis, R. Schulz, J.C. Smith, Simulation analysis of the temperature dependence of lignin structure and dynamics, *J. Am. Chem. Soc.* 133 (2011) 20277–20287.
- M.D. Smith, B. Mostofian, X. Cheng, L. Petridis, C.M. Cai, C.E. Wyman, J.C. Smith, Cosolvent pretreatment in cellulosic biofuel production: effect of tetrahydrofuran-water on lignin structure and dynamics, *Green Chem.* 18 (2016) 1268–1277.

- [47] T. Zou, N. Nonappa, M. Khavani, M. Vuorte, P. Penttila, A. Zitting, J.J. Valle-Delgado, A.M. Elert, D. Silbernagl, M. Balakshin, Experimental and Simulation Study of the Solvent Effects on the Intrinsic Properties of Spherical Lignin Nanoparticles, *J. Phys. Chem. B* 125 (2021) 12315–12328.
- [48] T.B. Rawal, M. Zahran, B. Dhital, O. Akbilgic, L. Petridis, The relation between lignin sequence and its 3D structure, *Biochim. Biophys. Acta Bioenerg.* 1864 (2020) 129547.
- [49] W. Li, S. Zhang, Y. Zhao, S. Huang, J. Zhao, Molecular docking and molecular dynamics simulation analyses of urea with ammoniated and ammoxidized lignin, *J. Mol. Graph. Model* 71 (2017) 58–69.
- [50] E.E. Brown, Minireview: recent efforts toward upgrading lignin-derived phenols in continuous flow, *J. Flow Chem.* 13 (2023) 91–102.
- [51] E. Melro, L. Alves, F.E. Antunes, B. Medronho, A brief overview on lignin dissolution, *J. Mol. Liq.* 265 (2018) 578–584.
- [52] P. Mäki-Arvela, I. Anugwom, P. Virtanen, R. Sjöholm, J.-P. Mikkola, Dissolution of lignocellulosic materials and its constituents using ionic liquids—a review, *Ind. Crop. Prod.* 32 (2010) 175–201.
- [53] H. Jiao, G. Xu, Y. Sang, H. Chen, Y. Li, Direct conversion of enzymatic hydrolysis lignin to cycloalkane fuel with hydrotalcite-derived Ni catalyst, *Catal. Today* 430 (2024) 114542.
- [54] Z. Luo, C. Liu, A. Radu, D.F. de Waard, Y. Wang, J.T. Behaghel de Bueren, P. D. Kouris, M.D. Boot, J. Xiao, H. Zhang, Carbon–carbon bond cleavage for a lignin refinery, *Nat. Chem. Eng.* 1 (2024) 61–72.
- [55] M. Yang, W. Zhao, S. Singh, B. Simmons, G. Cheng, On the solution structure of kraft lignin in ethylene glycol and its implication for nanoparticle preparation, *Nanoscale Advances* 1 (2019) 299–304.
- [56] B.G. Janesko, Modeling interactions between lignocellulose and ionic liquids using DFT-D, *Phys. Chem. Chem. Phys.* 13 (2011) 11393–11401.
- [57] W. Zhao, L.-P. Xiao, G. Song, R.-C. Sun, L. He, S. Singh, B.A. Simmons, G. Cheng, From lignin subunits to aggregates: insights into lignin solubilization, *Green Chem.* 19 (2017) 3272–3281.
- [58] L. Zhang, D. Zhao, M. Feng, B. He, X. Chen, L. Wei, S.-R. Zhai, Q.-D. An, J. Sun, Hydrogen bond promoted lignin solubilization and electrospinning in low cost protic ionic liquids, *ACS Sustain. Chem. Eng.* 7 (2019) 18593–18602.
- [59] Q. Li, Y. Dong, K.D. Hammond, C. Wan, Revealing the role of hydrogen bonding interactions and supramolecular complexes in lignin dissolution by deep eutectic solvents, *J. Mol. Liq.* 344 (2021).